Tuning Azoheteroarene Photoswitch Performance through Heteroaryl Design

Joaquín Calbo, Claire E. Weston, Andrew J. P. White, Henry S. Rzepa, Julia Contreras-García, Matthew J. Fuchter

Tuning Azoheteroarene Photoswitch Performance through Heteroaryl Design.

Joaquín Calbo[†,a] Claire E. Weston[†,b] Andrew J. P. White,[b] Henry S. Rzepa,[b] Julia Contreras-García*[,c,d] Matthew J. Fuchter*[,b]

[a] *Instituto de Ciencia Molecular, Universidad de Valencia, 46890 Paterna, Spain*

[b] *Department of Chemistry, Imperial College London, London SW7 2AZ, United Kingdom*

[c] *Sorbonne Universités, UPMC Univ Paris 06, UMR 7616, Laboratoire de Chimie Théorique, F-75005, Paris, France*

[d] *CNRS, UMR 7616, LCT, F-75005, Paris, France*

† Both authors contributed equally to this work

* contrera@lct.jussieu.fr, m.fuchter@imperial.ac.uk

Abstract

Photoswitchable compounds, which can be reversibly switched between two isomers by light, continue to attract significant attention for a wide array of applications. Azoheteroarenes represent a relatively new but understudied type of photoswitch, where one of the aryl rings from the conventional azobenzene class has been replaced with a five-membered heteroaromatic ring. Initial studies have suggested the azoheteroarenes – the arylazopyrazoles in particular – to have excellent photoswitching properties (quantitative switching and long *Z* isomer half-life). Here we present a systematic computational and experimental study to elucidate the origin of the long thermal half-lives and excellent addressability of the arylazopyrazoles, and apply this understanding to determine important structure-property relationships for a wide array of comparable azoheteroaryl photoswitches. We identify compounds with *Z* isomer half-lives ranging from seconds to hours, to days and to years, and variable absorption characteristics; all through tuning of the heteraromatic ring. Conformation perhaps plays the largest role in determining such properties; where the compounds with the longest isomerization half-lives adopt a T-shaped ground state *Z* isomer conformation and proceed through a T-shaped isomerization pathway, whereas the most complete photoswitching is achieved for compounds that have a twisted (rather than T-shaped) Z-isomer conformation. By balancing these factors, we report a new azopyrazole **3pzH**, which can be quantitatively switched to its *Z*-isomer (>98%) with 355 nm irradiation, near-quantitatively (97%) switched back to the *E* isomer with 532 nm irradiation, and has a very long half-life for

thermal isomerisation ($t_{1/2}$ = 74 d at 25 °C). Given the large tunability of their properties, the predictive nature of their performance, and the other functional opportunities afforded by usage of a heteroaromatic system, we believe the azoheteroaryl photoswitches to have huge potential in a wide range of optically addressable applications.

Introduction

Photoswitchable compounds, which can be reversibly switched between two isomers by light, continue to attract significant attention for a wide array of applications: from molecular motors, memory, and manipulators to solar thermal storage.[1] While there are several molecular properties that impact upon photoswitch performance, two are of central importance: (1) the completeness of photoswitching at a given wavelength of light, and (2) the thermal stability of each switched state. Among the classes of photochromic compounds studied, the azobenzenes maintain a privileged position due to the ease of their synthesis, their excellent photoswitching properties (such as high extinction co-efficient and quantum yields), and the fact that their isomerization results in a significant change in molecular shape.[2]

In general, a significant amount is known on how the chemical structure of photochromic compounds impacts their photochemical and thermal behavior.[1e,2-3] In the case of azobenzenes, excellent progress has been made in tuning the properties of azobenzenes via the substituents on the aromatic ring(s). For example, the past few years have seen the successful design of azobenzene photoswitches that can be addressed with visible light,[4] a property of particular importance for the rapidly growing field of photopharmacology.[5] Tetra-*ortho*-substituted azobenzenes have shown high promise in this regard, such as the *o*-methoxy analogues reported by Woolley[4a,6] and the *o*-fluoro compounds reported by Hecht.[4b,7] Both can be switched with visible light due to separation of the *n*-π* transitions of the *E* and *Z* isomers, which allows the *E* isomer to be switched at the long wavelength *n*-π* absorbance, rather than via the more usual π-π* transition (which generally requires UVA irradiation). In the case of the *o*-methoxyazobenzenes, separation of *n*-π* transitions is caused by a red-shift in the *E* isomer transition due to unfavorable electronic interactions between the lone pairs of the methoxy and azo moieties, which raises the *n*-orbital energy.[2b] Meanwhile for the fluoroazobenzenes, the separation of the *n*-π* transitions is caused by a blue-shift in the *Z* isomer transition due to a lowering of the *n*-orbital energy by the electron withdrawing fluorine substituents.[4b,8]

Increasing the thermal half-life of azobenzene *Z* isomers, while retaining good addressability[9], has arguably been the most challenging endeavor for this class of photoswitch. Apart from the cyclic azoaryl switches,[4d,10]

the *Z* isomers of azobenzenes are generally metastable and thermally revert back to the *E* isomer over time. Once again, the tetra-*ortho*-substituted azobenzenes have provided the optimum solution to this problem, with the *ortho*-fluoroazobenzenes reported to have (in addition to excellent addressability) *Z* isomer thermal half-lives of up to ca. 700 days (25 °C in DMSO).[4b,7] This property was rationalized computationally as being partially caused by the increased stability of the *Z* isomer, relative to the *E* isomer (vs azobenzene), and partially due to a contribution of *Z* isomer versus TS dipole moments.[4b,7]

We have recently reported an alternative approach to access azo photoswitches with excellent properties (quantitative switching and long *Z* isomer half-life) through replacement of one of the azobenzene aryl rings with a five-membered heteroaromatic ring.[11] Such heteroaryl azo compounds are far less well studied[12] than their ubiquitous azobenzene counterparts. Specifically, we found arylazopyrazoles (**4pzH** and **4pzMe**, Figure 1) to have excellent potential against the state of the art, as they could be quantitatively switched in one or both directions, depending on "*ortho*"-substitution,[13] and had half-lives of 10 and 1000 days at 25 °C. Given this performance, the arylazopyrazoles are beginning to be employed in applications including in supramolecular complexes[14] and as photopharmacological agents.[15] The performance of the azoheteroaryl photoswitches is very dependent on the nature of the heteroaromatic ring however, with the arylazopyrroles found to have shorter thermal half-lives (21 s and 12 h[16] for **2pyMe** and **2pyH** respectively, Figure 1) than the arylazopyrazoles;[11] some other heteroaryl azo compounds were found to have *Z* isomer half-lives of microseconds to nanoseconds.[12c] Clearly, a better understanding of how the photoswitching properties and performance can be tuned by a judicious choice of the type, positioning and substitution of the heteroaromatic ring would enable the azoheteroaryl photoswitches to reach their full potential. We note that such design 'rules' should not only allow for optimization of intrinsic photoswitch performance, but also for the realization of designs where the heteroaromatic ring provides other functional opportunities.[17]

There have been a large number of papers that use computational methods (see review by Burdette et al[2a]) to study the photochemical isomerization mechanisms of azobenzenes, although relatively few of these concern *Z*-*E* thermal isomerization.[18] Recently, Wegner and co-workers carried out experimental and computational studies into the thermal half-lives of sterically congested azobenzenes, and discovered that van der Waals forces play an important role.[18a] Favorable London dispersion interactions between *ortho*-alkyl substituents in the *Z* isomers are responsible for an increase in *Z* isomer stability upon increasing the bulkiness of the substituents. Comparatively, the azoheteroaryl photoswitches are almost unstudied in this regard.[11,19] Only very recently, the *Z*-*E* photoisomerization mechanism of two arylazopyrazoles has been computationally investigated.[20] Notably, one of these compounds was found to exhibit near stereospecific excited-state relaxation.

Herein we report a combined computational and experimental study on novel azoheteroaryl photoswitches derived from (nitrogen-based) five-membered heteroaromatic rings. We elucidate the origin of the long thermal half-lives and excellent addressability of the arylazopyrazoles, and apply this understanding to a wide array of comparable azoheteroaryl photoswitches. As such, we determine important structure-property relationships as a function of the type of heteroaromatic ring, the connectivity of the ring (relative to the azo group), and the ring substitution. Furthermore, we identify that calculation of the azo N=N Wiberg Index provides a quick and simple means to approximate the thermal half-live of this class of photoswitch, which can vary from seconds-days-months-years. This allows for rapid assessment of novel photoswitches based on ground state properties, importantly not relying on time-consuming transition state or excited state calculations. We believe these studies will greatly facilitate the further development of the azoheteroaryl photoswitches and their application to a broad array of functional areas.

Results and Discussion

Thermal half-lives of the Z-azoheteroaryl photoswitches

Elucidation of the factors underpinning the Z-isomer thermal half-life for the pyrrole and pyrazole-based photoswitches

We commenced our studies using the previously described[11] pyrrole and pyrazole photoswitches **2pyH**, **2pyMe**, **4pzH** and **4pzMe** (see Figure 1, and Table 1 for half-lives) as a small set of representative nitrogen-based azoheteroaryl photoswitches. Computational investigations were carried out in order to rationalize the structure-property relationships that had been observed experimentally, and to enable the discovery of other azoheteroaryl compounds with excellent photoswitching performance. Several conformations are available for such compounds, through rotation of the aromatic rings relative to the azo bridge. All the possible conformers of the *E* and *Z* isomeric forms were fully optimized using the hybrid exchange-correlation PBE0 functional[21] including the Grimme's dispersion correction in its latest version (D3)[22] and using the split-valence Pople's 6-31G** basis set.[23]

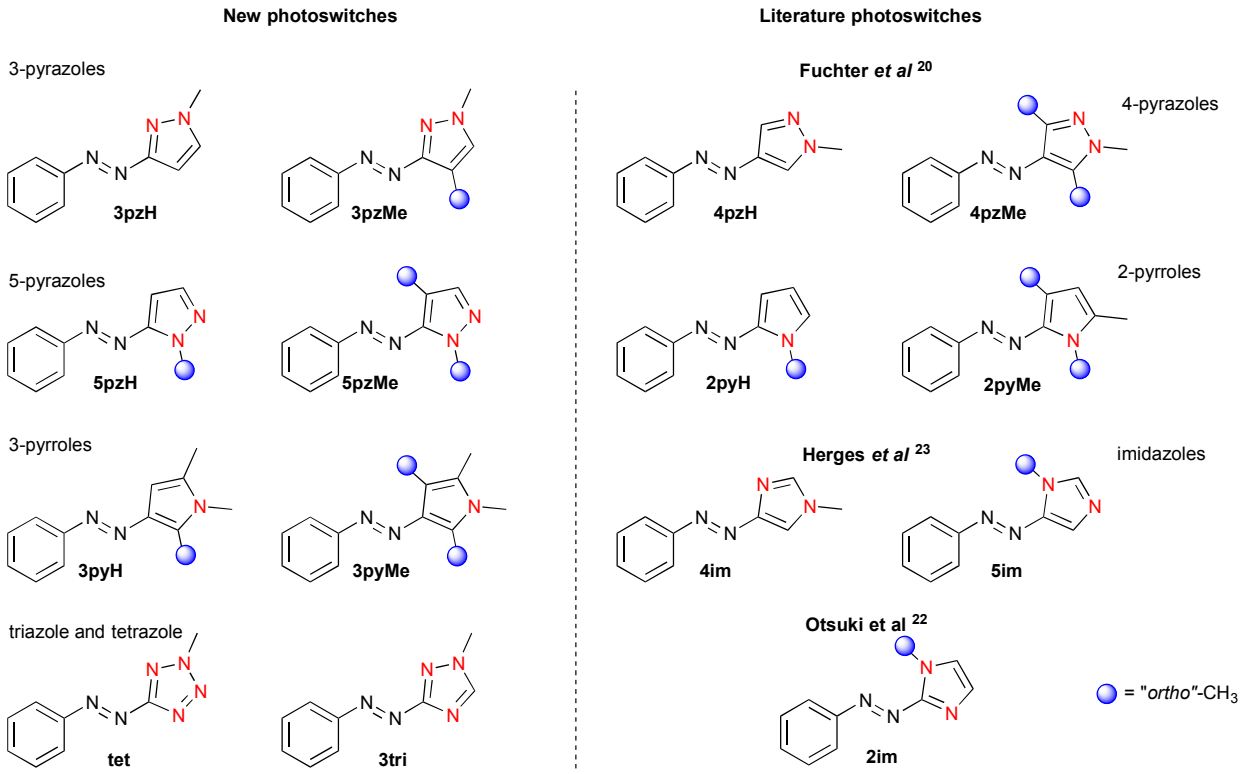

Figure 1. Azoheteroaryl photoswitches considered in this study.

Consistent with our previous study (Figure 1),[11] compounds such as **2pyH** and **4pzH**, which contain heteroaromatic rings that are not substituted in both the *ortho* positions, exhibit a *Z* isomer conformation with a perpendicular T shape (Figure 2a). Such a T-shaped conformation is only accessible for azo compounds with five-membered heteroaromatic rings, and not for conventional azobenzenes.[2a,12b] The introduction of bulky groups in both *ortho*-positions of the heteroaromatic ring (such as in **2pyMe** and **4pzMe**) disfavors the T-shaped conformation and instead a twisted conformation is predicted, which has been crystallographically characterized for **4pzMe**.[11] Compounds exhibiting twisted *Z* isomer conformations are observed experimentally to have shorter *Z* isomer half-lives relative to their less-hindered T-shaped analogues (Table 1).[11] By introducing only one methyl group into the *ortho* position, such as is the case for **2pyH**, the two possible conformers can coexist (Figure 2a), and so both T-shaped and twisted conformers need to be taken into account to provide accurate theoretical half-life times (*vide infra*).

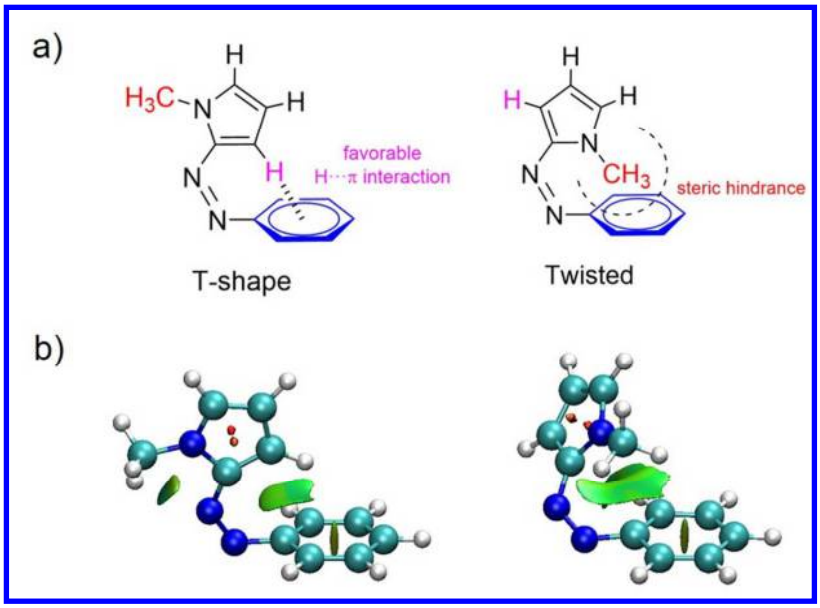

Figure 2. a) The two possible *Z* conformations when there is both a methyl group (bonded in this case to a nitrogen atom) and a hydrogen atom in the *ortho* positions, such as in **2pyH**. b) The corresponding NCI surfaces: green areas indicate weak non-covalent interactions whereas narrow red regions designate steric ring clashes.

From analysis of the relative enthalpies ($\Delta H_{Z\text{-}E}$) between the *E* and *Z* minimum-energy conformations, the *Z* isomer was found to be more than 10 kcal/mol less stable than the corresponding *E* isomer for all the compounds examined (see Table S1 in the Supplementary Information – SI). This difference increases upon introduction of two *ortho* methyls onto the heteroarene to ca. 13 kcal/mol, which provides a thermodynamic driving force for accelerated isomerization. Given this, it was postulated that the increase in *Z* isomer energy for **2pyMe** and **4pzMe** was due to a destabilization of the *Z* isomer ground state by the (sterically induced) twisted conformation. However, a closer inspection of the computed conformers reveals a subtle interplay of interactions, as can be visualized using a non-covalent index (NCI) analysis.[24] *Z* isomer stabilization of derivatives containing at least one *ortho*-hydrogen on the heteroarene (**2pyH** and **4pzH**) can occur through interactions present in the T-shaped conformation, which are absent in the bis-*o*-methylated compounds (**2pyMe** and **4pzMe**). A localized surface arises between the *ortho*-hydrogen and the benzene ring (Figure 2b), which indicates the presence of a favorable C-H···π interaction. As a reference, the interaction energy for a T-shaped benzene dimer at the PBE0-D3/6-31G** level is calculated to be 2.90 kcal/mol. However, the twisted conformations of the bis-*o*-methylated compounds (**2pyMe** and **4pzMe**) exhibit a greater attractive NCI surface as a result of a larger dispersive contribution, despite the increased steric repulsion experienced (Figure 2b). When computed through Grimme's D3 approach,[22] the dispersive contribution to the stability of the T-shaped *Z* isomer compounds **2pyH** and **4pzH** is ca. 8 kcal/mol, whereas it is ca. 11 kcal/mol in the case of the twisted methylated compounds **2pyMe** and **4pzMe** (see Table S1). For highly substituted azobenzenes,[18a] the dispersive contribution has been reported to overcome the steric repulsion and stabilize the *Z* isomer, increasing the isomerization half-life. Similarly, in the azoheteroaryl compounds, the computational investigation of heteroarene substituents more bulky than a methyl group was found to result in stabilizing dispersive interactions in

the *Z* isomer that surpass any steric congestion (see Table S2 and Figure S24 in the SI). Thus there appears to be a compensation principle in effect where the introduction of substituents destabilizes the structure through steric clashes, but the substituted ring adopts a conformation that maximizes mutual stabilizing dispersive interactions. Despite this, the destabilizing steric effect appears to dominate for the systems under primary study here (*ortho* H vs Me), with the (twisted) substituted heteroarene *Z* isomers (**2pyMe** and **4pzMe**) being higher in energy than comparable compounds with T-shaped *Z* isomer conformers (**2pyH** and **4pzH**).

The computed conformation-induced differences in the relative energies between *E* and *Z* isomers do not however correlate with the half-live trends observed experimentally (Table 1). For example, calculations of the free energy for *Z-E* isomerization indicate that the *Z* isomer of **4pzMe** is 15.8 kcal/mol less stable than the *E* isomer, whereas in **2pyH** the difference is slightly smaller (11.7 kcal/mol); however, the half-lives of the *Z* isomers of these compounds follow the opposite trend: 10 days and 12 hours, respectively. It would therefore appear that there is a significant kinetic component to the thermal isomerization rates observed.

Table 1. Theoretical thermodynamic and kinetic parameters including the free energy for the *Z-E* isomerization reaction ($\Delta G_{Z\text{-}E}$, kcal/mol) and the free energy barrier ($\Delta G^{\ddagger}$, kcal/mol) for the lowest energy conformer of each *Z*-isomer, and the weighted average half-life times (WA $t_{1/2}$) for all four possible TSs compared with the reported experimental values.

	$\Delta G_{Z\text{-}E}$	$\Delta G^{\ddagger}$ [a]	WA $t_{1/2}$	Experimental $t_{1/2}$
2pyH	-11.7	22.2 (II)	1.2 h	12 h [c]
2pyMe	-14.8	19.8 (II)	120 s	21 s [b]
4pzH	-11.5	26.4 (I)	108 days	1000 days [b]
4pzMe	-15.8	23.7 (I)	1 day	10 days [b]

[a] The type of the minimum-energy TS is indicated within parenthesis. [b] Data taken from Fuchter et al.[11] [c] Lit. value of 3 h reported by Fuchter et al[11] was measured at ~10^{-2} M (see further discussion below).

Given this, transition states (TS) and activation barriers ($\Delta G^{\ddagger}$) were computed for the different *Z-E* isomerization processes at the DFT PBE0-D3/6-31G** level of theory. Two principle mechanistic pathways for azobenzene isomerization have been previously reported – rotation about the N=N bridge and inversion at one of the azo nitrogen atoms – however, variations on these have also been suggested.[2a] In the case of azoheteroaryl photoswitches, the inversion mechanism was found to be the lowest energy pathway for the thermal isomerisation of all the compounds analyzed (see Figures S25 and S26 for further details). Inversion could occur either at the azo nitrogen bearing the phenyl ring (type-I, Figure 3a) or at the azo nitrogen bearing the heteroaryl ring (type-II). Moreover, and in accordance with the conformational possibilities afforded by these novel photoswitches, the type-I TS is reminiscent of the *Z* isomer ground state conformation, where the heteroaryl ring is (almost) perpendicular to the benzene ring, whereas the type-II TS is closer to the *E* isomer conformation, where the two aromatic rings are (almost) coplanar. Since there are two possible conformations for the inversion transition state when the system is non symmetric on either side of the azo group (Figure 3a), there are four possible transition states to be considered.

Analysis of all these TSs yielded, in general, similar energetic barriers for the four possible pathways. Changing the computational method, the basis set, or moving from the gas phase to a continuum solvent model for acetonitrile all had negligible effect on the computed relative energy barriers (Table S3). All the pathways were therefore weight-averaged to obtain mean half-lives according to a Boltzmann distribution of the TS energy barriers, assuming an equally-balanced ratio of the two *Z* conformers.[25] Theoretical evaluation of the free energy was carried out in gas phase, including thermal corrections to the total partition function at 298.15 K. Using transition state theory,[26] the rate constants for isomerization were calculated, assuming a first-order reaction, and from this we computed the final weighted-average half-lives (WA $t_{1/2}$ in Table 1). Despite the reasonably small energy differences (in the range of few kcal/mol) calculated for the transition state barriers of the different compounds, large differences in the half-lives for the photoswitches are predicted, which show good agreement with the available experimental data (Table 1).

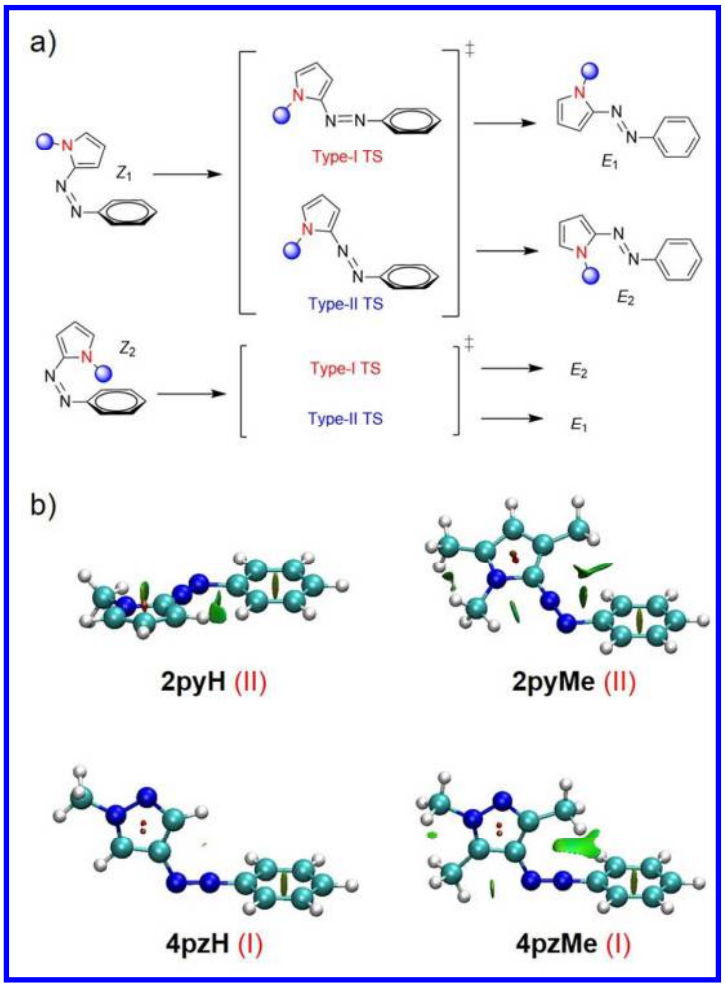

Figure 3. a) The two lowest energy *Z*-*E* thermal isomerization pathways of the representative photoswitch **2pyH**; b) NCI surfaces calculated from the PBE0-D3/6-31G** electron density for the TS of compounds **2pyH**, **2pyMe**, **4pzH** and **4pzMe** that lead to the lowest free energy barriers. The TS type (either I or II) is indicated within parenthesis.

NCI analysis was employed to disentangle the effects underpinning this energetic ordering. Pyrroles **2pyH** and **2pyMe** exhibit the lowest TS energy barriers and a TS similar to the *E* isomer conformation, where the two aromatic rings attempt to adopt a coplanar relationship (type-II). The presence of the *ortho* methyl group in **2pyMe** results in more significant twisting away from such co-planarity relative to **2pyH**. The NCI surfaces of the pyrrole TS (Figure 3b) show a number of stabilizing dispersive interactions. For example, when quantified through Grimme's approach, we find the stabilizing dispersive contribution to compound **2pyMe** to be 10.2 kcal/mol, compared with a smaller value of 7.1 kcal/mol for **2pyH**. The lowest-energy TS for pyrazoles **4pzH** and **4pzMe** has a T-shaped conformation, similar to the *Z* isomer ground state conformation, where the heteroaryl ring is perpendicular to the phenyl ring (type-I). Interestingly, NCI analysis indicates dispersion is almost absent in the (lowest-energy) TS of **4pzH** (Figure 3b); the dispersive contribution is calculated to be only 6.2 kcal/mol (see Table S1). As in the case of the ground state conformations, methyl substitution at the *ortho* position leads to greater dispersive effects. These results suggest that the TSs are stabilized by non-covalent interactions, mainly dispersion, and such interactions determine the TS energetics: compound **2pyMe** has the highest stabilization through dispersion and therefore the lowest energy barrier, whereas compound **4pzH** has the lowest dispersion stabilization and therefore the highest TS energy.

In summary, the isomerization rate (and therefore the half-lives) of photoswitches **2pyH**, **2pyMe**, **4pzH** and **4pzMe** are controlled by both the *Z* isomer ground state stabilization and the TS energy for a given isomerization process. In general, the pyrazoles appear to have much longer isomerization half-lives than the pyrroles due to their preference to adopt T-shaped (type-I) TSs, which lack significant dispersive stabilization and hence have a higher TS energy. Methyl substitution in the *ortho* position twists the ground state *Z* isomer conformations of both the pyrroles and pyrazoles away from the T-shape which, through steric effects, destabilizes the ground state *Z* isomer of **2pyMe** and **4pzMe** relative to **2pyH** and **4pzH,** respectively. The compound with the longest thermal *Z* isomer half-life, **4pzH** (1000 days), exhibits both a T-shaped ground state *Z* isomer conformation and proceeds through a T-shaped isomerization pathway. The role of the T-shape conformation in these processes is therefore crucial.

Synthesis and characterization of new azoheteroaryl photoswitches

In order to elucidate structure-property relationships for a wider array of azoheteroaryl photoswitch systems and provide predictive trends to enable future azoheteroaryl photoswitch design, it was necessary to synthesize and characterize a larger number of analogues (Figure 1). These were considered in comparison with **2pyH**, **2pyMe**, **4pzH** and **4pzMe**, and with the phenylazoimidazole photoswitches previously characterized in the literature.[12a,12b] The principle variables considered when selecting novel candidate compounds for synthesis were: i) the number and positioning of the nitrogen atoms (and therefore formally the heteroaryl ring present); and ii) the number and positioning of heteroaryl methyl substituents. The new analogues (Figure 1) were synthesized using similar routes to those previously described (see SI).[11]

Table 2. Experimental *Z*-*E* thermal isomerisation kinetics at 25 °C, including the re-measured values for literature compounds **2pyH**, **4im** and **5im**.

	Position of azo on heteroarene		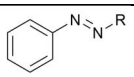	Rate (k) / s^{-1}	Half-life ($t_{1/2}$)
tetrazole	4	**tet** [a]	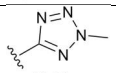	2.1×10^{-7}	39 d
triazole	3	**3tri** [a]	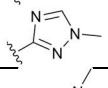	3.8×10^{-7}	21 d
pyrazoles	3	**3pzH** [a]	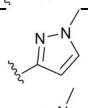	1.1×10^{-7}	74 d
	3	**3pzMe** [b]	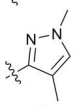	1.5×10^{-6}	5.8 d
	4	**4pzH** [a,e]	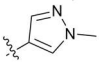	7.6×10^{-9}	1000 d
	4	**4pzMe** [b,e]	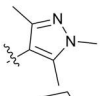	7.7×10^{-7}	10 d
	5	**5pzH** [b]		7.4×10^{-7}	11 d
	5	**5pzMe** [c]		1.6×10^{-5}	12 h
pyrroles	2	**2pyH** [c,f]		6.5×10^{-5}	12 h
	2	**2pyMe** [c,d,e]	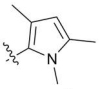	3.3×10^{-2}	21 s
	3	**3pyH** [c,d]	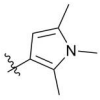	2.2×10^{-6}	3.7 d
	3	**3pyMe** [c,d]	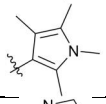	7.6×10^{-4}	0.25 h
imidazoles	2	**2im** [g]		2.2×10^{-5}	9 h
	4	**4im** [c,h]		3.3×10^{-6}	2.4 d
	5	**5im** [c,i]		1.2×10^{-6}	6.5 d

Measured using [a] NMR at a range of elevated temperatures, ~10^{-2} M in d_6-DMSO; [b] NMR, ~10^{-2} M in d_3-MeCN; [c] UV-vis, 10^{-5} M in anhydrous MeCN. [d] Rates obtained were dependent on the water content of solvent. [e] Reported by Fuchter et al[11]. [f] Lit. value of 3 h reported by Fuchter et al[11] was measured at ~10^{-2} M. [g] Reported by Otsuki et al[12a]. [h,i] A thermal half-life of 5 h[h] and 22 d[i] (solvent or concentration not known) was reported by Herges et al[12b].

Thermal isomerization rates and half-lives were measured for the *Z* isomers of the newly synthesized compounds (Table 2, which includes the literature compounds for comparison). Following *E*-*Z* switching at 355 nm (*vide infra*),

rates at 25 °C were obtained using either UV/vis or NMR spectroscopy (Figures S15-18): The kinetics of analogues with half-lives of less than 1 day (or those showing a concentration-dependence – *vide infra*) were measured using UV/vis spectroscopy at a concentration of 1 x 10^{-5} M in acetonitrile. Otherwise, kinetics were more conveniently measured by NMR spectroscopy at ~10^{-2} M; either at 25 °C in d_3-acetonitrile or, for analogues with half-lives of longer than 10 days at 25 °C, (for example **tet**, **3tri**, **3pzH**), at a range of higher temperatures (70 – 110 °C) in DMSO-d_6. For the latter cases, $\Delta H^{\ddagger}$ and $\Delta S^{\ddagger}$ values were extracted using Eyring plots, and from these, the isomerization rates and half-lives at 25 °C were calculated (see SI).

Clear experimental trends are apparent from the data summarized in Table 2. When comparing compounds with the same azo linkage position on a given heteroarene series, the bis-*ortho*-methylated photoswitches had faster thermal isomerisation rates than their singly or non-methylated analogues, consistent with the analysis above. The position of the ring nitrogen atom(s) also had a significant effect on the rate. By separating the photoswitches into those with ≤ 1 *ortho*-hydrogens and those with two *ortho*-hydrogens, the 2-azopyrroles had shorter half-lives than the corresponding 3-azopyrroles ($t_{1/2}$: **2pyMe** < **3pyMe, 2pyH** < **3pyH**), and for the azopyrazoles, the 5-analogues had the shortest half-lives and the 4-analogues had the longest half-lives ($t_{1/2}$: **5pzH** < **3pzH** < **4pzH**, **5pzMe** < **3pzMe** < **4pzMe**). It should be noted that although **3pzMe** has been included in the **pzMe** series, it differs from the other compounds (**5pzMe** and **4pzMe**) in that it has only one *ortho*-methyl and a basic nitrogen in the other *ortho*-position (as opposed to two *ortho*-methyls). The finding that this compound fits into the **pzMe** series suggests that *ortho* basic nitrogens have a similar effect on the thermal isomerisation rate as *o*-methylation. Consistent with this, the presence of a nitrogen atom in the *ortho* position was computationally found to disfavor the T-shaped conformation, and results in a twisted conformation of the *Z* isomer (Figure 4). For the imidazole compounds, **4im** and **5im** both have one *ortho*-hydrogen so can be considered as part of the same series ($t_{1/2}$: **5im** > **4im**) due to the formation of a T-shaped conformation (as discussed by Herges and co-workers).[12b] **2im** however has one *ortho*-methyl and one *ortho* basic nitrogen so adopts a twisted conformation.

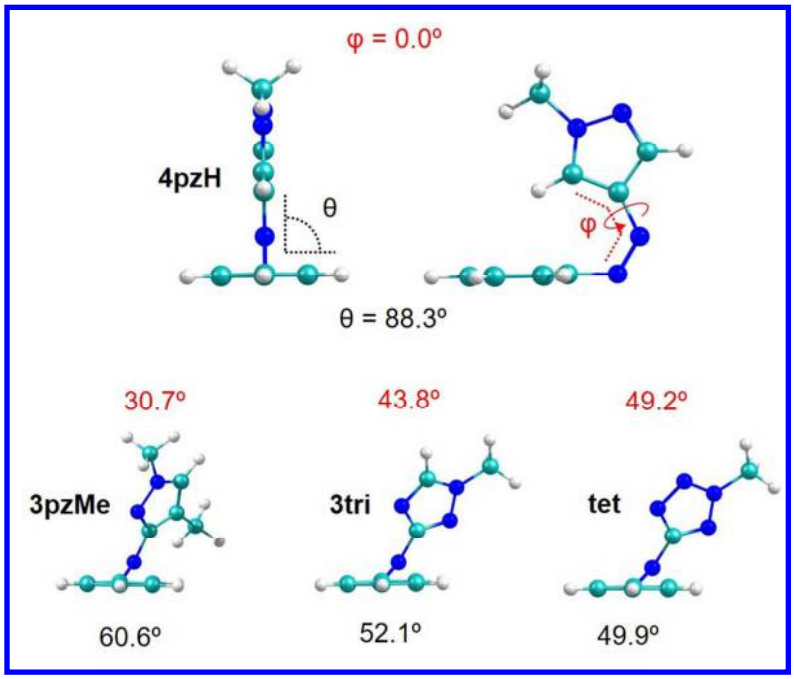

Figure 4. Characteristic dihedral angles of the lowest energy conformations of representative *Z* isomer compounds with basic nitrogen atoms in the *ortho* position of the heteroarene (bottom) compared with the long-living T-shaped *Z* isomer of photoswitch **4pzH** (top).

More extensive structure property relationships: Computational vs experimental trends

An analogous computational treatment to that described for compounds **2pyH**, **2pyMe**, **4pzH** and **4pzMe** was performed on all the newly synthesized compounds, as well as the other previously reported azoheteroaryl photoswitches in the literature. Comparison of the *Z-E* isomerization half-lives obtained experimentally to those computed (taking into account both thermodynamic and kinetic factors) is shown in Figure 5. In general, the calculated half-lives were good predictions of the experimental values (i.e. within the same order of magnitude), and the majority of half-lives were predicted in the correct order, shortest to longest (Figure 5). The comparison of the theoretical vs experimental half-lives for this larger array of compounds confirms the physical effects (outlined above) that underpin the thermal half-life of these azoheteroaryl photoswitches: compounds that adopt a more T-shaped conformation, such as **3pyH** and **5pzH**, had slower thermal isomerisation rates than their twisted analogues (**3pyMe** and **5pzMe**). In addition to this, the effect seen upon changing the position of the azo linkage on the heteroarene was correctly predicted for the pyrroles and pyrazoles, with the sole exception of **3pzMe**. Experimentally, the order of increasing half-life for this series was **5pzMe** < **3pzMe** < **4pzMe**, whereas the calculated half-life for **3pzMe** was longer than **4pzMe**. As discussed above, this compound differs from the other azopyrazoles studied as it has one *ortho*-methyl and one *ortho* basic nitrogen, rather than two *o*-methyls or one *o*-methyl and one *ortho* CH group. The azo-positional effect can be rationalized by the extent of conjugation between the heteroarene and the phenylazo moiety (*vide infra*).

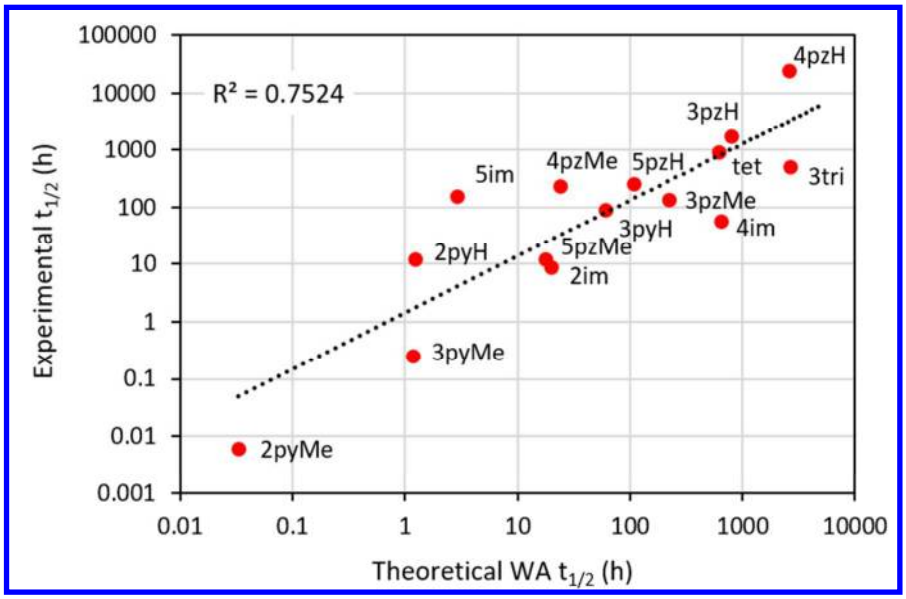

Figure 5. Comparison between the theoretical vs experimental half-life times for the list of photoswitches under study.

In our initial comparison of the experimental and computed half-lives, there were two compounds (**4im** and **5im**) – previously reported by Herges and co-workers[12b] – for which the predicted values were observed to be notably more divergent than the experimental values obtained from the literature. Since there was no apparent reason why these compounds in particular should be outliers, combined with the fact that the concentrations or solvents in which half-lives were measured were not reported, we decided to synthesize **4im** and **5im** and re-measure their thermal half-lives. The compounds were synthesized following the literature method reported by Herges.[12b] Confirmation of the structures of isomeric compounds **4im** and **5im**, including unambiguous assignment of **4im** by X-ray crystallography (see Figure S2 in the SI), was consistent with the previous structural assignment.[12b] An interesting effect was observed however when attempts were made to determine the thermal isomerization rates of **4im** and **5im**: the measured rate of **4im** was concentration-dependent, with faster rates observed at high concentrations (>>10^{-4} M) (Table 2). Although the origin of this effect is unclear, it seems that there may be bimolecular pathways at higher concentration that facilitate isomerization for this compound. At concentrations below 10^{-3} M, no concentration dependence on the half-life was observed. **5im** did not show a concentration dependence; however, under the conditions of this study (10^{-5} M concentration in acetonitrile, 25 °C) a shorter half-live was obtained than that previously reported.[12b] The half-lives for **4im** and **5im**, when measured at the same concentration of the majority of the other photoswitches included in this study (10^{-5} M, see Table 2) were 2.4 d and 6.5 d, respectively (c.f. the reported values of 5 h and 22 d, which were presumably carried out under different conditions). The inclusion of these revised values into our comparative analysis gave an improved fit (Figure 5).

In light of the discovery of a concentration-dependence on the thermal half-life, we examined whether other compounds under study exhibited a comparable effect. To complete the azoimidazole series, **2im** was also synthesized and found to have the same half-life when measured at 10^{-5} M (by UV/vis) and at 10^{-2} M (by NMR),

which matched the value reported by Otsuki and co-workers ($t_{1/2}$ of 9 h).[12a] For the novel photoswitches synthesized in this study, a representative set[27] were examined and it was found that the azopyrroles show a concentration dependence, whereas the azopyrazoles do not (see Figures 19-23 in the SI for more details). Specifically, the published half-life of **2pyH** was 3 hours when recorded at ~10^{-2} M and 12 hours when measured at 10^{-5} M, whereas it shows negligible concentration dependence at concentrations below ~10^{-3} M. This observation is crucial when designing new photoswitches and envisaging their technological use: concentration may be a useful parameter for tuning switch properties.

It was also found that the azopyrroles are sensitive to water content in the solvent (as reported previously for **2pyMe**[28]), whereas the other heteroaryl systems were not; where increased water content leads to accelerated thermal isomerisation. Although the origin of this effect has not been further studied, it is plausible that polar isomerization transition states are more stabilized in the presence of water, thus leading to faster isomerization. The fact that pyrroles are good electron donors (σ_{Ar}^{+} = -1.96 for *N*-methyl-2-pyrrolyl)[29] into the azophenyl moiety may lead to the formation of a more polar TS for heteroaryl photoswitches. Theoretical calculations confirmed that the pyrrole-based transition states have larger electron-donor character than the pyrazole analogues, and that this difference is more accentuated upon inclusion of water solvent effects (Figure S27).

Rapid approximation of Z-isomer thermal half-life

While in-depth computational study of the thermodynamics and kinetics of the isomerization process provides insight into the structural-property effects of the azoheteroaryl photoswitches, and allows for assessment of the magnitude of the *Z* isomer thermal half-life, such an analysis clearly requires TS structures to be obtained; which is not practical for large screening of diverse sets of prospective new heteroaromatic photoswitch designs. We therefore sought to define a predictive metric that would be simpler/quicker to calculate and inform on likely photoswitch performance. We selected calculation of the N=N bond order (the Wiberg index[30] or WI) of the optimized *Z* conformers as a potentially useful metric. Bond orders were calculated as the sum of the off-diagonal square of the density matrix obtained at the PBE0-D3/6-31G** level (see the SI for more details), and averaged for the two possible *Z* isomer conformations of each photoswitch. As expected, the WIs obtained show a linear correlation with respect to the azo N=N bond length (Figure S28a). In all systems studied, the N(azo)-C(benzene) bond length is computed to be larger than the N(azo)-C(heteroarene) bond length. The difference between these two magnitudes (NC asymmetry)[18f] is also predicted to correlate with the N=N bond length (Figure S28b). Since the N=N bond length highly depends on the extent of π-conjugation in the photoswitch, WI calculations will give valuable information on the strength of the N=N double bond and, presumably, on the relative half-life times.

Compounds that exhibit a twisted Z isomer conformation, due to *ortho*-substitution, were found to result in elongation of both the N-C hindered bond, and the N=N azo bond, with a concomitant decrease in the bond order

(smaller Wiberg index). This was particularly noticeable for the bis-*o*-methylated **2pyMe** and **4pzMe** when compared to their less hindered analogues **2pyH** and **4pzH** (Figure 6). The nature and connectivity of the heteroaromatic ring was found to impact more noticeably on the Wiberg index calculated. For example, the 2-pyrroles have lower Wiberg indices (e.g. **2pyH**, and **2pyMe**) than the 3-pyrroles and all of the pyrazoles. The effect upon changing the connectivity of the heteroaryl ring (or conversely viewed as changing the azo positioning) can be qualitatively explained in terms of conjugative electron donation from the *N*-methyl lone pair to the azophenyl system (Figure 6). For the 2-azopyrroles and the 5-azopyrazoles, the position of the *N*-methyl relative to the azo group allows more extensive conjugation of the lone pair into the azophenyl relative to the other regioisomers. This improved electron donation from the heteroaryl ring likely leads to a decrease in the bond order through polarization of the N=N bond (push-pull type effect). Similar electronic effects are apparent upon changing the type of heteroaryl ring: for example, pyrroles (σ_{Ar}^{+} = -1.96, *N*-methyl-2-pyrrolyl)[29] are better electron donors into the azo group than pyrazoles (σ_{Ar}^{+} = -0.41, -0.99, -0.29 for *N*-methyl-3-pyrazolyl, *N*-methyl-4-pyrazolyl, and *N*-methyl-5-pyrazolyl respectively),[31] and hence have lower Wiberg indices (bond orders) relative to the pyrazoles.

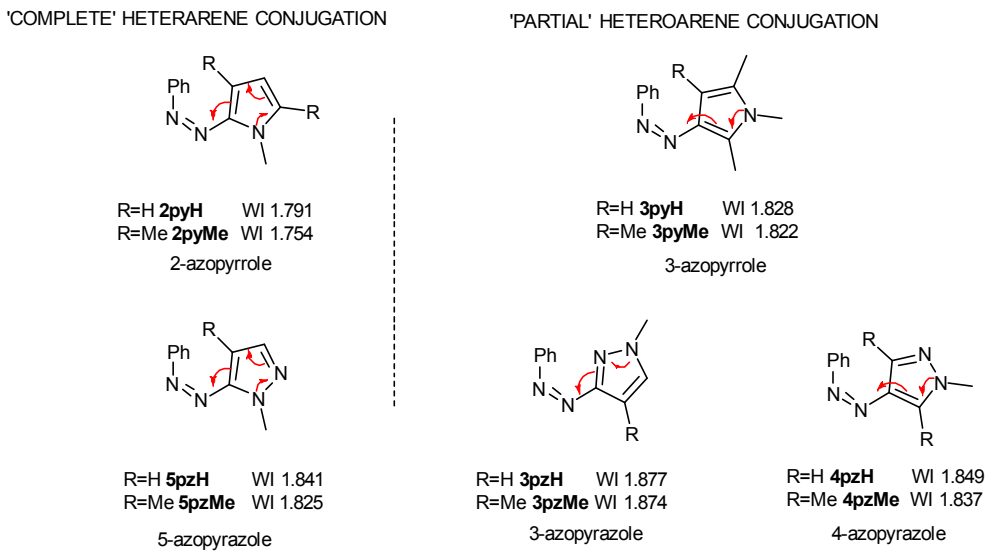

Figure 6. Conjugation of the heteroarene into the azophenyl moiety.

Comparison of the experimental $t_{1/2}$ values with the Wiberg indices for all the azoheteroaryl photoswitches studied is shown in Figure 7. Despite the simplified nature of the Wiberg index to approximate the structural and conformational effects of this diverse range of compounds, a clear trend appears, although residuals are significant (R^2 = 0.54). When compared with the theoretical half-life times, the correlation is more significant (R^2 = 0.82, see Table S4 and Figure S29). Photoswitches with 'partial' heteroarene conjugation (Figure 6), such as **3pzH**, **3tri**, **tet**, etc., are predicted to provide the largest Wiberg indices, correlating well with long experimental half-lives. On the other hand, 'complete' heteroarene conjugated systems, such as **2pyH**, **2pyMe**, **5pzMe**, are calculated with the

lowest Wiberg indices out of the compounds studied, which correlates well with their short half-life values. The largest outliers in this trend are those most impacted by *ortho* substitution or lack thereof. For example, photoswitch **4pzH** has a calculated half-life two orders of magnitude larger than expected from its Wiberg index. As discussed above, its lack of *ortho* substitution allows for a T-shaped *Z* isomer ground state and T-shaped TS barrier. In contrast, photoswitch **3pyMe** exhibits a half-life nearly two orders of magnitude shorter than what is expected from its Wiberg index. In this case, the bis-*ortho*-substitution more significantly destabilizes the *Z* isomer with respect to the transition state, permitting an unexpectedly fast *Z*-*E* isomerization (see also compound **2pyMe**). Other key outliers include those with concentration dependent half-lives, such as **2pyH** and **5im**. We note that when **4pzH**, **2pyH**, and **5im** are removed from the comparison, the trend with respect to experimental $t_{1/2}$ values vs the Wiberg index is much improved (R^2 = 0.76).

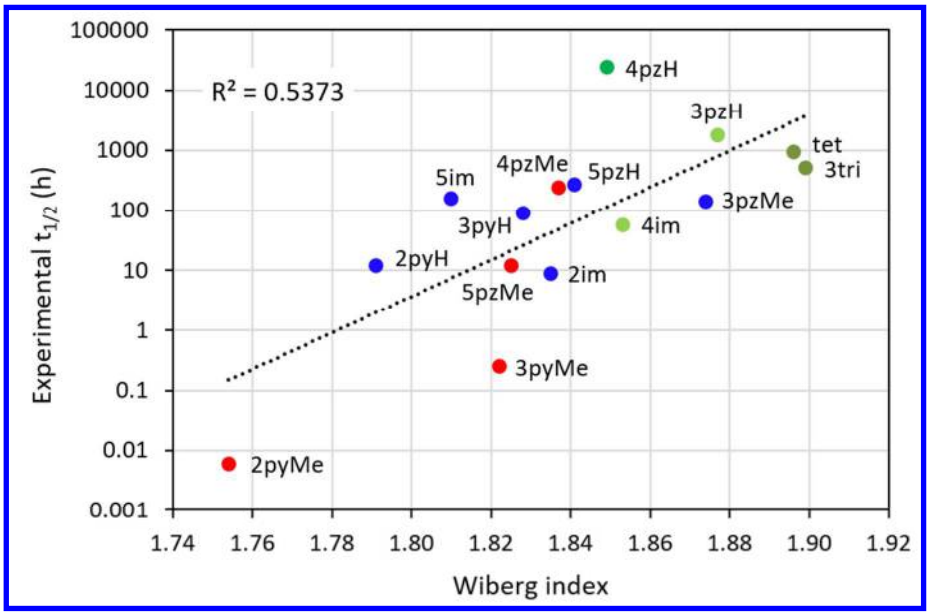

Figure 7. Correlation between the experimental half-lives and the Wiberg index colored by families: bis-*ortho*-methylation (red), mono-*ortho*-methylation (blue), and no *ortho*-methylation (green). The last family is subdivided in the number of sp^2 nitrogen atoms in *ortho*-position (light – one atom, medium – zero atoms, and dark – two atoms).

Z-*E* photoisomerization

The UV/vis absorbances of azoarene *E* and *Z* isomers determines their practical utility: their addressability.[9] Overlapping absorbances in the characteristic electronic transitions between such isomers leads to incomplete photoswitching. Therefore, suitable separation of the λ_{max} values for transitions associated with each isomer is highly desirable for good/quantitative two-way photoswitching at defined wavelengths. The low-energy *n*-π* band is often exploited for *Z*-*E* photoisomerisation of azobenzenes; however, there is frequently overlap of the absorbances between the two isomers in this spectral window. Several modified azobenzenes, such as Woolley's *o*-methoxy[4a,6a]

and Hecht's *o*-fluoroazobenzenes,[4b,7] have been reported in which the *n*-π* band of the two isomers are sufficiently well separated to allow photoswitching for both *E*-*Z* and *Z*-*E* isomerization using this transition. In particular, several of the *o*-fluoroazobenzene analogues developed by Hecht have improved (near quantitative) photoconversion (≤95% *Z* and ≤97% *E*) to those usually seen for azobenzenes.[7]

In our initial study,[11] we showed that the nature (pyrrole versus pyrazole) and ring (methyl) substitution of four azoheteroaryl compounds significantly impacts their absorption spectra and, in turn, their photoswitching behavior. Most notably, we found that excitation of the π-π* transition of *E*-**4pzMe** at 355 nm resulted in complete photoswitching (>98% *Z* isomer), whereas irradiation of the tail of the *n*-π* absorbance of *Z*-**4pzMe** switched it back to >98% *E* isomer. Thus, **4pzMe** could be quantitatively switched in both directions, a result which surpassed all of the state-of-the-art azo switches.[11] While **4pzMe** additionally exhibited an impressive thermal half-life for the *Z* isomer (10 days), compound **4pzH** was found to be the best performing photoswitch of the initial study in terms of *Z* isomer half-life (~1000 days, *vide supra*). Conversely, less efficient (*Z* to *E*) switching was possible for **4pzH**, due to an overlap of the *Z* and *E* isomer *n*-π* absorbances. Given the increased understanding developed above for the features of the azoheteroaryl switches that impact thermal half-life, we sought to develop comparable understanding of changes in isomer specific transitions, and thus obtain a clear design rationale for how to obtain heteroazoaryl switches with *both* excellent two-way photoswitching and *Z*-isomer thermal half-life.

Frontier molecular orbital analysis

First, we analyzed the energy of the frontier molecular orbitals responsible of the lowest-lying singlet excited states for the *Z* and *E* isomers of the heteroazoaryl photoswitches. Given that two different conformations are possible for each isomer, the frontier molecular orbitals (FMO) of each isomer were calculated at the PBE0-D3/6-31G** level of theory for both conformers, in all cases. Figure 8 shows representative HOMO, HOMO-1 and LUMO frontier MOs for **2pyH**. Both *E* isomer conformations are planar, and differ only in the rotational orientation of the heteroaromatic ring, relative to the azophenyl group. These two conformations have very similar HOMO and LUMO levels and topologies (see Figure 8), indicating that the relative orientation of the heteroarene, and thus the *E* isomer conformation, does not have a dramatic effect on the frontier MOs (Figure S30). The HOMO and LUMO of the *E*-isomer are clearly of a π-nature whereas the HOMO-1 is an *n*-type orbital.[32] The conformation of the *Z* isomer had a much more dramatic effect on the frontier MOs. While the symmetry of the HOMO and HOMO-1 mostly shows mixed *n*/π character for the *Z* isomer conformers, compounds able to form an orthogonal T-shaped conformation (Figure 8) result in a more clearly defined *n*-type HOMO and a π-type HOMO-1 orbital due to symmetry constraints. The LUMO in all the *Z* isomers is of a π nature.

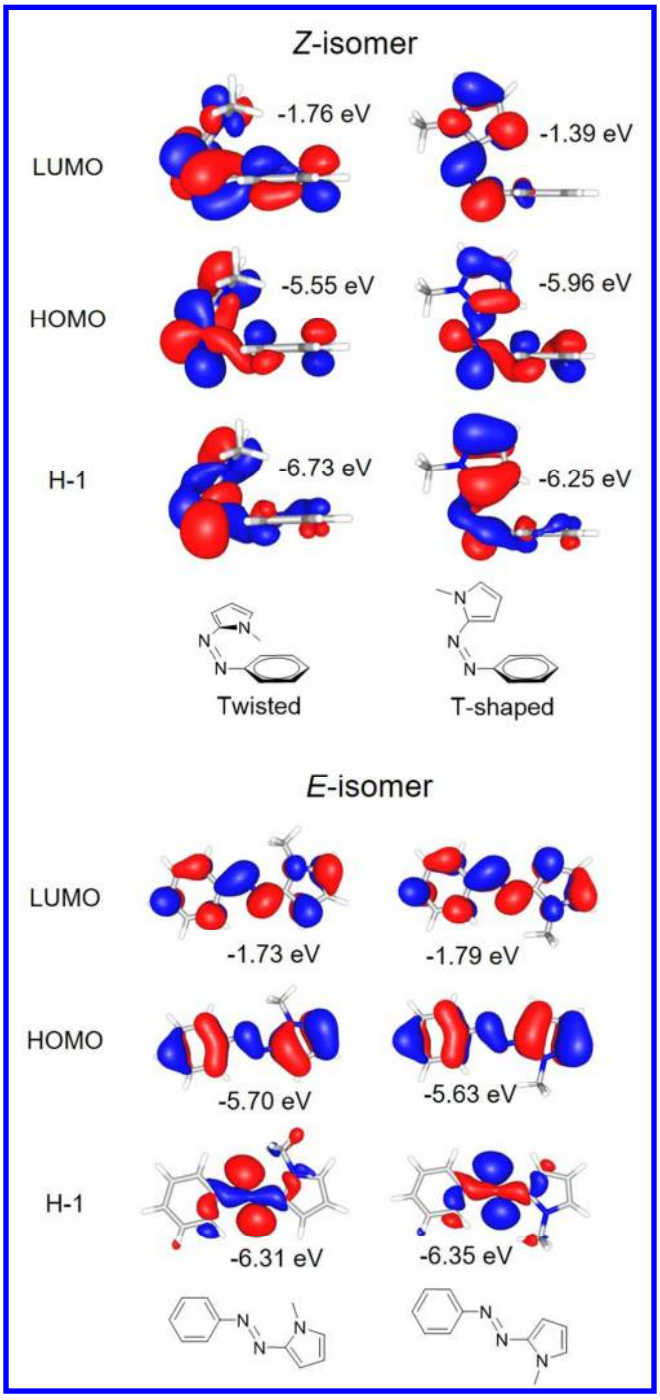

Figure 8. Frontier molecular orbitals of the representative photoswitch **2pyH** in the minimum-energy orientations for *Z* (top) and *E* isomers (bottom).

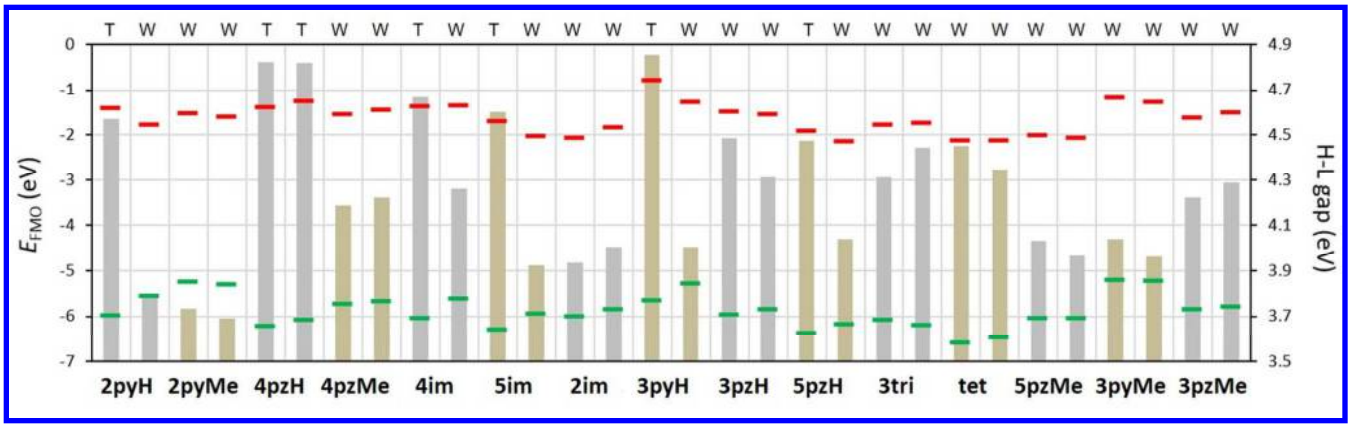

Figure 9. Frontier molecular orbital (FMO) diagram for the *Z* isomers. FMO energies are plotted as green (HOMO) and red (LUMO) lines, with the computed energy given by the left-hand side axis. HOMO-LUMO energy gaps are displayed as bars, with the computed energy given by the right-hand side axis. Each compound is associated with two sets of data which correspond to the two possible conformers. Twisted and T-shaped arrangements are labelled as W and T, respectively.

The significant variation in *Z* isomer frontier MOs energy levels, as a function of conformation, can clearly be observed across the series in Figure 9, in contrast to that found for the *E* isomer (Figure S30). For the *Z* isomers, the photoswitches that experience the largest differences in the FMO energy between the two conformers are *Z*-**2pyH**, **4im**, **5im**, **3pyH** and **5pzH**. These compounds contain one substituted *ortho* position (either N-Me, C-Me or a basic N lone pair) and one unsubstituted position (C-H). As such, they can exhibit either a twisted or a T-shaped conformation (see Figure 8 for **2pyH**). In the T-shaped conformation, the *n*-orbital is stabilized while the π*-orbital becomes higher in energy, resulting in a considerable increase of the HOMO-LUMO energy gap.

Following this analysis, we sought to correlate the frontier molecular orbitals with their associated electronic transition energy. The 20 lowest-lying singlet excited states were computed for each conformer under the time-dependent density functional theory (TDDFT) framework[33] at the PBE0/6-31G** level. The reliability of the PBE0 functional was assessed by comparison with other popular hybrid functionals (see Tables S5-S8 in the SI).[34] The frontier molecular orbital gaps were compared to the associated electronic transition energies in order to analyze the amount of monodeterminantal character of the most important excited states in *Z* and *E* isomers (see SI). For the *E* isomers, the azoheteroarene photoswitches follow a linear correlation between the S_1 energy and the H-1–L gap (Figure S31a), suggesting that this transition is best described by the one-electron promotion for the H-1 to the LUMO. The H-1 is the typical *n*-type lone pair orbital for the azo group (Figure 8). We note that while the ground state is usually well represented by a single Slater-determinant, the excited state often consists of several determinants.[35] Thus, depending on the mixture of configurations, the size of the two electron-terms and the orbital energy differences, the H → L transition is not necessarily the lowest in energy.[36] The S_2 transition for the *E* isomer, in turn, corresponds to the H → L electronic transition, with a linear correlation between the S_2 energy and the H–L gap (Figure S31b). For the Z-isomers, the lowest-lying S_1 excited correlates excellently with the H–L gap in all

compounds (Figure S32a); the correlation being indicative of the monodeterminantal character of this electronic transition. Conversely, the S_2 excited state is calculated as being multiconfigurational, showing a poor correlation with the H-1 → L gap (Figure S32b). This analysis shows that care should be taken in the analysis of optical transitions relative to HOMO-LUMO energies.

Experimental photoswitching

In order to provide a larger experimental dataset to compare with this computational analysis, UV/vis spectra and photoswitching experiments were recorded for each of the new photoswitches in acetonitrile. Since the best photoconversions were generally achieved with 355 nm (*E*-*Z*) and 532 nm (*Z*-*E*) irradiation, these wavelengths were principally used in the switching experiments (see Table 3). Azopyrazole *E*-**5pzH** could be quantitatively switched to its *Z* isomer using 355 nm irradiation, while the majority of other compounds were switched to photostationary states (PSSs) containing a mixture of isomers. *Z*-**3pyMe** could be near-quantitatively (98%) switched back to its *E* isomer using 532 nm, while the majority of other compounds gave PSSs containing a mixture of isomers, due to overlapping absorbances between *E* and *Z* isomers at this wavelength. Notably however, one of the azopyrazoles newly synthesized for this study - *E*-**3pzH** - could be quantitatively switched to its *Z*-isomer (>98%) with 355 nm irradiation and near-quantitatively (97%) switched back to the *E* isomer with 532 nm irradiation. Theoretical calculations for *Z*-**3pzH** predict conformers slightly distorted from a perfectly T-shaped disposition (Figure S33), resulting in an increased oscillator strength for the *n*-π* transition compared to, e.g., the analogous **4pzH** system (Table 3), thus allowing improved switching at 532m for *Z*-**3pzH**. This, combined with its long half-life for thermal isomerisation ($t_{1/2}$ = 74 d at 25 °C), makes it an extremely desirable photoswitch (i.e. comparable photoconversions to **4pzMe**,[11] but with increased *Z* isomer thermal stability). PSS compositions and extracted *Z* isomer spectra (Figures S11 and S12), were determined as described in the SI (and as demonstrated in Figures S4 to S10). From this, absorption maxima (λ_{max}) and molar extinction coefficients (ε) were obtained for the π-π* and *n*-π* absorbances of both isomers of each compound (Table 3).

Table 3. Photostationary states and spectral data for the azoheteroarenes.

Photostationary states	*E isomer* π-π*	*E isomer n*-π*	*Z isomer* π-π*	*Z isomer n*-π*

	E-*Z* (% *Z*)	*Z*-*E* (% *E*)	λ_{max} / nm	$10^{-2} \times \varepsilon$ / M^{-1} cm^{-1}	λ_{max} / nm	$10^{-2} \times \varepsilon$ / M^{-1} cm^{-1}	λ_{max} / nm	$10^{-2} \times \varepsilon$ / M^{-1} cm^{-1}	λ_{max} / nm	$10^{-2} \times \varepsilon$ / M^{-1} cm^{-1}
tet	76 ± 2	72 ± 3	310	167 ± 15	442	3.73 ± 0.34	~290	24.3 ± 2.2 [b]	428	10.1 ± 0.92 [b]
3tri	90 ± 2	84 ± 3	310	187 ± 22	438	5.05 ± 0.59	272	48.9 ± 5.7 [b]	434	12.7 ± 1.5 [b]
3pzH	> 98	97 ± 3	320	146 ± 17	425	7.78 ± 0.91	272	90.8 ± 11	422	10.8 ± 1.3
5pzH	> 98	79 ± 3	341	162 ± 20	425	6.76 ± 0.8	289	69.4 ± 8.4	430	8.73 ± 1.1
3pzMe	96 ± 2	87 ± 3	325	174 ± 20	428	6.12 ± 0.72	286	51.5 ± 6.0 [b]	438	13.6 ± 1.6 [b]
5pzMe	94 ± 2	86 ± 3	340	186 ± 21	435	8.54 ± 0.95	296	55.3 ± 6.2 [b]	451	22.1 ± 2.5 [b]
3pyH	77 ± 3	85 ± 5	363	193 ± 18	~410 [a]	- [a]	311	87.5 ± 7.9 [c]	405	14.2 ± 1.3 [c]
3pyMe	85 ± 3	98 ± 2	345	166 ± 15	~410 [a]	- [a]	300	52.0 ± 4.6 [c]	462	33.2 ± 2.9 [c]
2pyMe[d]	85 ± 3 [g]	>98	394	282 ± 18	~430 [a]	- [a]	346	70.4 ± 5.7 [c]	479	60.8 ± 4.5 [c]
2pyH[d]	84 ± 2 [g]	82 ± 3	385	221 ± 18	~413 [a]	- [a]	333	162 ± 13 [b]	423	15.7 ± 1.3 [b]
4pzMe[d]	>98	>98	335	227 ± 18	425	9.63 ± 0.76	296	57.7 ± 4.6	441	23.0 ± 1.8
4pzH[d]	>98	70 ± 3	328	166 ± 13	417	6.40 ± 0.51	275	80.6 ± 6.4	403	6.66 ± 0.53
2im[e]	>98 [h]	-	363	170	~450	12.6	-	-	-	-
4im[f]	>95 [i]	-	336	148	-	-	-	-	-	-
5im[f]	98 [i]	45 [j]	362	258	-	-	-	-	-	-

The position of the band (λ_{max} in nm) and the corresponding extinction coefficient (ε in M^{-1} cm^{-1}) are indicated. See SI for UV/vis spectra. [a] *n*-π* absorbance appears as a shoulder on the π-π* absorbance, hence ε cannot be obtained. [b,c] These values are for the extracted ([b]) or estimated ([c]) pure *Z* isomer. [d] Literature values reported by Fuchter et al.[11] [e] Literature values reported by Otsuki et al.[12a] [f] Literature values reported by Herges et al.[12b] All *E*-*Z* PSSs were measured at 355 nm irradiation except for the following which were measured at: [g] 415 nm; [h] 363 nm; [i] 365 nm. All *Z*-*E* PSS were measured at 532 nm irradiation except for the following which was measured at: [j] 455 nm irradiation.

n–π electronic transition*

TDDFT calculations were used to further rationalize the experimental results obtained, and in light of the analysis above. Each conformer was treated independently, and the effect of the conformation (T-shaped, twisted, etc.) was analyzed throughout. In the planar azoheteroarene *E* isomers, a mirror plane exists through the plane generated by the azo function (for both conformers), and therefore the *n*–π* transition becomes symmetry-forbidden at the equilibrium geometry. Indeed, negligible intensity is computed for the *n*-π* (H-1 → L) transition of the *E* isomer (Table S5). Persico and co-workers[37] reported that the intensity of the *n*-π* absorption band for *E*-azobenzene depends on the effect that vibrational motions have on the electronic structure. Therefore, the anharmonicity, the

thermal distributions, and the solvent effects all have to be taken into account. Vibrational and rotational motion leads to a population of molecules away from the equilibrium geometry, which provide weakly allowed *n*-π* transitions and correspondingly a small absorbance. This rationale is clearly also relevant for azoheteroarenes, with a weak *n*-π* transition observed experimentally for the *E* isomers of all the compounds studied (Table 3).

The *Z* isomer *n*-π* (H → L) transition, on the other hand, is computed from weak to moderately intense, depending on the photoswitch and conformation under analysis (Table S6). The most important feature affecting the magnitude of the *n*-π* band intensity in the *Z* isomer is the potential to form a T-shaped conformation. In the perfect T-shaped conformer, as in the planar *E* isomer, a mirror plane exists through the plane of the azo function and, therefore, the transition becomes symmetry-forbidden at the equilibrium geometry. As a result, all the compounds with the azoheteroaryl group orthogonal to the benzene ring (CCNN dihedral ≈ 90°, T-shaped) are computed to have a singlet S_1 excitation with negligible oscillator strength (Figure 10). Conversely, the photoswitches that cannot adopt a T-shaped conformation exhibit an S_1 state with oscillator strengths up to f = 0.090. The correlation of the CCNN dihedral angle to the computed intensity of the *n*-π* transition, for all the photoswitches studied, can be seen in Figure 10. Such conformation-induced tuning of the magnitude of the *n*-π* transition intensity is clearly observable from the experimental data. For example, the *Z* isomers of photoswitches with two *ortho*-methyls on the heteroarene (**5pzMe**, **3pyMe**) cannot adopt a T-shaped conformation (*vide supra*), and therefore had a considerably larger *n*-π* absorbance than their non- or singly *o*-methylated analogues (Table 3). Likewise, the presence of two heteroaryl basic nitrogens adjacent to the azo group (**tet**, **3tri**), or one basic nitrogen and one *ortho*-methyl (**3pzMe**), increased the intensity of the *Z* isomer *n*-π* band relative to that of the *E* isomer (Table 3), due to an increasingly twisted conformation. Since the T-shaped conformation is additionally responsible for an increased H-L band gap (*vide supra*), compounds exhibiting such a conformation in their *Z* isomer should result in a shift of the *n*-π* band to higher energies. Experimentally this is indeed the case – for example, the λ_{max} for the *n*-π* transitions of *Z*-**3pyH** and *Z*-**5pzH** occur at shorter wavelengths than those of *Z*-**3pyMe** and *Z*-**5pzMe**, respectively.

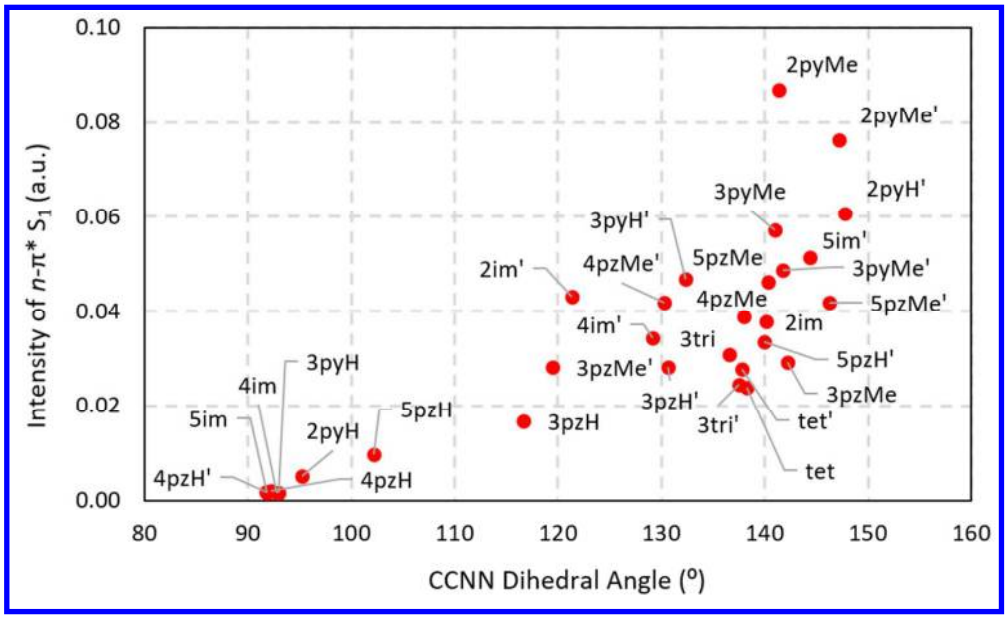

Figure 10. Correlation between the intensity of the lowest-lying S_1 excited state of *n*-π* nature with respect to the dihedral between the benzene and the azo group in the *Z* isomer. The two possible conformers for each isomer are included.

An increase in the number of N atoms is predicted to result in a systematic stabilization of the HOMO and LUMO for the *Z* isomers, and a global decrease in the HOMO-LUMO gap (Figure 9). When comparing the *Z*-isomers of **3pzH**, **4pzH**, **4im**, **3tri** and **tet**, there is a general decrease in energy of the *n*-π* electronic transition upon increasing the number of N atoms as calculated by TDDFT (Table S6). For example, the *n*-π* electronic excitation is predicted to change from 409 nm in **4pzH** to 455 nm in **3tri,** although little difference is found moving to **tet** (453 nm). This trend is supported by the experimental data: λ_{max} = 403, 434, and 428 nm for **4pzH**, **3tri** and **tet**, respectively. In terms of conjugation effects resulting from heteroaryl connectivity, a consistent shift of the *n*-π* (H → L) transition to longer wavelengths was predicted for compounds going from 'partial' to 'complete' heteroarene conjugation (Table S6 and Figure 6). For instance, the *n*-π* excitation of 'partial'-conjugated 3-azopyrroles **3pyH** and **3pyMe** is calculated at 438 and 473 nm, respectively, which moves to 458 and 490 nm for the 'complete'-conjugated 2-azopyrroles **2pyH** and **2pyMe**. This also holds for the 'partial'-conjugated 3- (**3pzH** and **3pzMe**) and 4-azopyrazoles (**4pzH** and **4pzMe**) compared to the 'complete'-conjugated 5-pyrazole compounds (**5pzH** and **5pzMe**). These trends are in excellent agreement with the experimental position of the *n*-π* band in the *Z* isomers gathered in Table 3.

π-π electronic transition*

For the majority of the compounds studied, the π-π* electronic transition of the *E* isomer was computed to exhibit a moderately intense absorbance band with oscillator strength *f* = 0.5 – 0.9. Since the π-π* electronic transition of the *E* isomers is assigned to a HOMO to LUMO transition (H → L), the computed H-L band gap trends can be compared

to the λ_{max} position of the *E* isomer π-π* transition. When comparing compounds where the N-Me group is located in the same position relative to the azo linkage (**3pzH** vs **3tri** vs **tet**), a systematic increase in the energy of the π-π* transition is computed as the number of nitrogen atoms increases: from 3.99 eV (311 nm) in **3pzH** to 4.09 eV (303 nm) in **tet**. When considering compounds with two nitrogen atoms in the heterocyclic ring, but positioned differently (**4pzH** vs **4im** vs **3pzH**), the π-π* bands of **4pzH** and **4im**, were predicted to have comparable π-π* transition energies of 315 and 319 nm (3.94 and 3.89 eV) respectively, both lower than **3pzH**, which has a calculated transition energy of 311 nm (3.99 eV). These trends are supported by the experimental data, although, as for the *n*-π* band, little/no difference is observed for **3tri** versus **tet**: λ_{max} = 336, 328, 320, 310, and 310 nm for *E*-**4im**, **4pzH**, **3pzH**, **3tri** and **tet** respectively. The π-π* band of **3pyMe** and **3pyH** was less red-shifted than for the 2-azopyrrole analogues (**2pyMe** and **2pyH**); a result of 'partial' versus 'complete' conjugation of the azo group with the heteroarene (see Figure 6). For similar reasons, the 5-azopyrazole analogue **5pzH** had red-shifted π-π* absorbances relative to the 3-azopyrazole and 4-azopyrazole analogues (**3pzH** and **4pzH**), while a small red-shift was seen for bis(*o*-methylated) 5-azopyrazole *E*-**5pzMe** relative to 4-azopyrazole *E*-**4pzMe**. The calculated data are in excellent agreement with the experimental trends for the 3-, 4- and 5-azopyrazoles, whereas the significant conformational-dependence of the π-π* S_2 band position (Table S5) hinders a full comparison between 3- and 2-azopyrroles.

Band separation

Given that the extent of photoswitching in the PSS is primarily a function of the overlap of bands in the absorption spectrum, and the corresponding intensity of the relevant transitions, it is important to fully understand the structure-property relationships that underpin band separation. While the discussion above individually compares the position and intensity of the main *n*-π* and π-π* transitions as a function of both the azoheteroaryl photoswitch and isomer dependent conformations, a comparison of the computed versus experimental band separation is warranted. Such a comparison is shown in Table 4. In general, the computed band separations qualitatively correlate with those observed experimentally. By comparing compounds with and without *ortho*-methyl substitution, a significant enhancement especially of the *Z*-*E* photoconversion is achieved when substituting the *ortho* H by a methyl group. For instance, % *Z*-*E* photoconversion increases from 84, 85, 70 and 79% in **2pyH**, **3pyH**, **4pzH** and **5pzH**, respectively, to >98, 98, >98 and 86% for **2pyMe**, **3pyMe**, **4pzMe** and **5pzMe** (Table 4). This improvement in the photoconversion efficiency is a result of *n*-π* band separation between *Z* and *E* isomers, which increases upon moving from H-substituted to methyl-substituted photoswitches (Table 4), a result of the effect of the increasingly twisted conformation of the Z-isomer (*vide supra*). In the case of **4pzH**/**4pzMe**, inversion of the *n*-π* band positions between *E* and *Z* is found both experimentally and theoretically. Pyrrole heteroaromatic switches show in general poorer *E*-*Z* photoconversion efficiencies with respect to the pyrazole analogues, a result of the difference between the *n*-π* band of the *Z* isomer and the π-π* of *E* isomer (Table 4). For example, the experimental *n*-π*(*Z*) minus π-π*

(*E*) difference is recorded to increase from 42 nm in **3pyH** to 102 nm in **3pzH**, thus explaining the *E*-*Z* photoconversion improvement from 77 to >98%.

While intrinsically good band separation enables improved photoswitching, judicious choice of the irradiation wavelength, particularly to spectral regions significantly outside of the absorption maxima, can allow for further improvement in the completeness of photoswitching (albeit with a decrease in quantum yield). A key case in point in this study is photoswitch **3pzH**. Using light at 532 nm (the *n*-π* λ_{max} of *Z*-**3pzH** is 422 nm), excellent *Z*-*E* photoisomerisation was achieved for **3pzH** (97% *E*), although a relatively long irradiation time (~15 minutes) was required to reach the PSS. We tentatively assign this to a difference in oscillator strengths between *E* and *Z* isomers for **3pzH** at 532 nm: the *Z*-**3pzH** conformation (which is slightly distorted from a perfectly T-shaped disposition - Figure S33) results in an increased oscillator strength for the *n*-π* transition at 532 nm compared to the planar *E*-**3pzH**. Thus, once again, the chemical structure and conformation of the potential photoswitch can help us comprehend and design compounds that can achieve better photoconversions.

Table 4. Experimental and theoretical separation (values in nm are given as *Z* minus *E*) of the *n*-π* and π-π* bands for the *Z* and *E* isomers.

Compound	*n*-π* separation (*Z* – *E*)		π-π* separation (*Z* – *E*)		*n*-π* (*Z*) – π-π* (*E*)	
	experimental	theoretical[a]	experimental	theoretical[a]	experimental	theoretical[a]
2pyH	10	16	-52	-38	38	113
2pyMe	49	50	-48	-29	85	135
4pzH	-14	-38	-53	-36	75	94
4pzMe	16	15	-39	-30	106	141
4im	--	-15	--	-28	--	127
5im	--	8	--	-29	--	119
2im	--	22	--	-11	--	145
3pyH	-5	-9	-52	-32	42	90
3pzH	-3	-13	-48	-19	102	143
5pzH	5	6	-52	-23	89	135
3tri	-4	-25	-38	-23	124	135
tet	-14	-28	-20	-16	118	152
5pzMe	16	28	-44	-12	111	150
3pyMe	51	22	-46	-9	115	148
3pzMe	10	-2	-39	-6	113	117

[a] Theoretical band separation for the isomers was calculated by taking the simple average band position between the two conformers for a given isomer.

Conclusions

We present a systematic computational and experimental study on the azoheteroarene photoswitches: photochromic azoaryl molecules consisting of one five-membered heteroaromatic ring and one benzene ring. Modification of the type of the heteroaromatic ring, as well as its positioning (relative to the azo group) and substitution has been found to have a huge effect on the performance of this class of switch. This is most notable in the *Z* isomer thermal half-life data, where we identify compounds with half-lives ranging from seconds to hours, to days and to years. In depth computational study has revealed the thermal *Z*-*E* isomerization rate to be determined by both thermodynamic (*Z*-*E* isomer relative stability) and kinetic (activation barrier) factors, which are, in turn, influenced by the structure and conformation of the photoswitch in question. Conformation perhaps plays the largest role, where the compounds with the longest isomerization half-lives adopt a T-shaped ground state *Z* isomer conformation and proceed through a T-shaped isomerization pathway. Non-covalent interaction analysis can readily explain the stabilization or destabilization of such conformations.

Conversely, the most complete photoswitching is achieved for compounds that have a twisted (rather than T-shaped) Z-isomer conformation; where such a conformation is achieved through the use of substituents or basic nitrogen atoms in the *ortho* positions. Such twisting particularly results in an increase in oscillator strength for the *n*-π* band of the Z-isomer and therefore allows for the selection of wavelengths that can selectively address each isomer. Ultimately, to achieve complete bidirectional photoswitching and a long *Z* isomer half-life, a balance must be found between these two conformational states. In this study, such a balance is exemplified by the newly discovered azopyazole **3pzH**, which can be quantitatively switched to its *Z* isomer (>98%) with 355 nm irradiation, near-quantitatively (97%) switched back to the *E* isomer with 532 nm irradiation, and has a very long half-life for thermal isomerisation ($t_{1/2}$ = 74 d at 25 °C). *Z*-**3pzH** has a conformation only slightly distorted from a perfectly T-shaped disposition (Figure S33), which retains the slow thermal isomerization of the *Z* isomer, but results in an increased oscillator strength for the *n*-π* transition compared to, e.g., the analogous **4pzH** system.[11]

We also show the Wiberg index to be suitably useful as a predictive measure for estimating thermal half-lives, allowing for large numbers of compounds to be screened without the need to obtain free energies for the *E* and *Z* isomer conformations and TSs, which have high computational cost. Although outliers are present in our analysis, which limit quantitative comparison, our data (see Figure 8) clearly shows that assessment of the Wiberg index gives a useful 'first approximation' as to whether a given switch is likely to have a short, medium or long half-life. As such, this should allow identification of photoswitches that would be suited to particular applications, where either short or long thermal half-lives may be required.

Given the large tunability of their properties, the predictive nature of their performance, and the other functional opportunities[15,17a] afforded by usage of a heteroaromatic system, we believe the azoheteroaryl photoswitches to

have huge potential in a wide range of optically addressable applications. The approaches hereby presented provide a means to rationally and rapidly design novel photoswitches to achieve a given performance requirement.

Supporting Information Available. Text, tables, figures, and CIF files giving synthetic methods, NMR and crystallographic data, photochemical methods including additional spectra and kinetics, and computational details. This material is available free of charge via the Internet at http://pubs.acs.org. Raw data files are openly available at DOI: 10.6084/m9.figshare.4287302.

Acknowledgements. MJF and CEW thank the Engineering and Physical Sciences Research Council for funding. JC acknowledges the Spanish Ministry of Education, Culture, and Sport (MECD) for an FPU grant. We also thank Dr Kuimova (Imperial College London) for equipment access.

References

(1) a) Gostl, R.; Senf, A.; Hecht, S., *Chem. Soc. Rev*. **2014**, *43*, 1982-1996. b) Bléger, D.; Hecht, S., *Angew. Chem. Int. Ed*. **2015**, *54*, 11338-11349. c) Szymański, W.; Beierle, J. M.; Kistemaker, H. A. V.; Velema, W. A.; Feringa, B. L., *Chem. Rev*. **2013**, *113*, 6114-6178. d) Feringa, B. L.; Browne, W. R. *Molecular Switches*; VCH: Weinheim, 2011. e) Russew, M.-M.; Hecht, S., *Adv. Mater*. **2010**, *22*, 3348-3360. f) Kucharski, T. J.; Ferralis, N.; Kolpak, A. M.; Zheng, J. O.; Nocera, D. G.; Grossman, J. C., *Nat Chem* **2014**, *6*, 441-447. g) Zhitomirsky, D.; Cho, E.; Grossman, J. C., *Adv. Energy Mater*. **2016**, *6*, 1502006. h) Feng, Y.; Liu, H.; Luo, W.; Liu, E.; Zhao, N.; Yoshino, K.; Feng, W., *Sci. Rep.* **2013**, *3*, 3260. i) Saydjari, A. K.; Weis, P.; Wu, S., *Adv. Energy Mater.* **2016**, 1601622.

(2) a) Bandara, H. M. D.; Burdette, S. C., *Chem. Soc. Rev*. **2012**, *41*, 1809-1825. b) Beharry, A. A.; Woolley, G. A., *Chem. Soc. Rev*. **2011**, *40*, 4422-4437.

(3) a) Bastianelli, C.; Caia, V.; Cum, G.; Gallo, R.; Mancini, V., *J. Chem. Soc., Perkin Trans. 2* **1991**, 679-683. b) Irie, M.; Fukaminato, T.; Matsuda, K.; Kobatake, S., *Chem. Rev*. **2014**, *114*, 12174-12277. c) Feng, W.; Luo, W.; Feng, Y., *Nanoscale* **2012**, *4*, 6118-6134. d) Luo, W.; Feng, Y.; Cao, C.; Li, M.; Liu, E.; Li, S.; Qin, C.; Hu, W.; Feng, W., *J. Mater. Chem. A* **2015**, *3*, 11787-11795.

(4) a) Beharry, A. A.; Sadovski, O.; Woolley, G. A., *J. Am. Chem. Soc*. **2011**, *133*, 19684-19687. b) Bléger, D.; Schwarz, J.; Brouwer, A. M.; Hecht, S., *J. Am. Chem. Soc*. **2012**, *134*, 20597-20600. c) Yang, Y.; Hughes, R. P.; Aprahamian, I., *J. Am. Chem. Soc*. **2012**, *134*, 15221-15224. d) Siewertsen, R.; Neumann, H.; Buchheim-Stehn, B.; Herges, R.; Näther, C.; Renth, F.; Temps, F., *J. Am. Chem. Soc*. **2009**, *131*, 15594-15595.

(5) a) Velema, W. A.; Szymanski, W.; Feringa, B. L., *J. Am. Chem. Soc*. **2014**, *136*, 2178-2191. b) Broichhagen, J.; Frank, J. A.; Trauner, D., *Acc. Chem. Res*. **2015**, *48*, 1947-1960.

(6) a) Samanta, S.; Beharry, A. A.; Sadovski, O.; McCormick, T. M.; Babalhavaeji, A.; Tropepe, V.; Woolley, G. A., *J. Am. Chem. Soc*. **2013**, *135*, 9777-9784. b) Samanta, S.; McCormick, T. M.; Schmidt, S. K.; Seferos, D. S.; Woolley, G. A., *Chem. Commun*. **2013**, *49*, 10314-10316.

(7) Knie, C.; Utecht, M.; Zhao, F.; Kulla, H.; Kovalenko, S.; Brouwer, A. M.; Saalfrank, P.; Hecht, S.; Bléger, D., *Chem. Eur. J*. **2014**, *20*, 16492-16501.

(8) Other successful attempts to red shift azo photoswitch absorbance include through BF_2-coordination. See e.g. Refs. 4c and Yang, Y.; Hughes, R. P.; Aprahamian, I., *J. Am. Chem. Soc*. **2014**, *136*, 13190-13193.

(9) van Dijken, D. J.; Kovaříček, P.; Ihrig, S. P.; Hecht, S., *J. Am. Chem. Soc*. **2015**, *137*, 14982-14991.

(10) Hammerich, M.; Schütt, C.; Stähler, C.; Lentes, P.; Röhricht, F.; Höppner, R.; Herges, R., *J. Am. Chem. Soc*. **2016**, *138*, 13111-13114.

(11) Weston, C. E.; Richardson, R. D.; Haycock, P. R.; White, A. J. P.; Fuchter, M. J., *J. Am. Chem. Soc.* **2014**, *136*, 11878-11881.

(12) a) Otsuki, J.; Suwa, K.; Narutaki, K.; Sinha, C.; Yoshikawa, I.; Araki, K., *J. Phys. Chem. A* **2005**, *109*, 8064-8069. b) Wendler, T.; Schütt, C.; Näther, C.; Herges, R., *J. Org. Chem.* **2012**, *77*, 3284-3287. c) Garcia-Amorós, J.; Díaz-Lobo, M.; Nonell, S.; Velasco, D., *Angew. Chem. Int. Ed.* **2012**, *51*, 12820-12823.

(13) Substitution at one or both of the positions of the 5-member heteroarene adjacent to the azo group are referred to as "ortho" throughout. Although this is not formally the correct usage of the term, it allows for simple comparison with the ortho-substituted azobenzenes.

(14) Stricker, L.; Fritz, E.-C.; Peterlechner, M.; Doltsinis, N. L.; Ravoo, B. J., *J. Am. Chem. Soc.* **2016**, *138*, 4547-4554.

(15) Weston, C. E.; Kraemer, A.; Colin, F.; Yildiz, Ö.; Baud, M. G. J.; Meyer-Almes, F.-J.; Fuchter, M. J., *ACS Infect. Dis.* **2016**, DOI: 10.1021/acsinfecdis.1026b00148.

(16) Value reported in this work.

(17) a) Weston, C. E.; Richardson, R. D.; Fuchter, M. J., *Chem. Commun.* **2016**, *52*, 4521-4524. b) Schütt, C.; Heitmann, G.; Wendler, T.; Krahwinkel, B.; Herges, R., *J. Org. Chem.* **2016**, *81*, 1206-1215.

(18) a) Schweighauser, L.; Strauss, M. A.; Bellotto, S.; Wegner, H. A., *Angew. Chem. Int. Ed.* **2015**, *54*, 13436-13439. b) Wang, Y.-P.; Zhang, Z.-X.; Xie, M.; Bai, F.-Q.; Wang, P.-X.; Zhang, H.-X., *Dyes Pigments* **2016**, *129*, 100-108. c) Ikegami, T.; Kurita, N.; Sekino, H.; Ishikawa, Y., *J. Phys. Chem. A* **2003**, *107*, 4555-4562. d) Wazzan, N. A.; Richardson, P. R.; Jones, A. C., *Photochem. Photobiol. Sci.* **2010**, *9*, 968-974. e) Dokić, J.; Gothe, M.; Wirth, J.; Peters, M. V.; Schwarz, J.; Hecht, S.; Saalfrank, P., *J. Phys. Chem. A* **2009**, *113*, 6763-6773. f) Cembran, A.; Bernardi, F.; Garavelli, M.; Gagliardi, L.; Orlandi, G., *J. Am. Chem. Soc.* **2004**, *126*, 3234-3243.

(19) Nabati, M., *J. Phys. Theor. Chem. IAU Iran,* **2016**, *12*, 325–338.

(20) Wang, Y.-T.; Liu, X.-Y.; Cui, G.; Fang, W.-H.; Thiel, W., *Angew. Chem. Int. Ed.* **2016**, DOI: 10.1002/anie.201607373.

(21) Adamo, C.; Barone, V., *J. Chem. Phys.* **1999**, *110*, 6158-6170.

(22) Grimme, S.; Antony, J.; Ehrlich, S.; Krieg, H., *J. Chem. Phys.* **2010**, *132*, 154104.

(23) Francl, M. M.; Pietro, W. J.; Hehre, W. J.; Binkley, J. S.; Gordon, M. S.; Defrees, D. J.; Pople, J. A., *J. Chem. Phys.* **1982**, *77*, 3654-3665.

(24) a) Johnson, E. R.; Keinan, S.; Mori-Sánchez, P.; Contreras-García, J.; Cohen, A. J.; Yang, W., *J. Am. Chem. Soc.* **2010**, *132*, 6498-6506. b) Contreras-García, J.; Johnson, E. R.; Keinan, S.; Chaudret, R.; Piquemal, J.-P.; Beratan, D. N.; Yang, W., *J. Chem. Theory Comput.* **2011**, *7*, 625-632.

(25) Assuming a 50% population of each conformer was found to give a comparable correlation between theoretical and experimental half-life times to a Boltzmann distribution of the two possible Z conformers.

(26) Eyring, H., *J. Chem. Phys.* **1935**, *3*, 107-115.

(27) Only compounds with half-lives of less than 1 day at rt (**2pyH**, **3pyH**, **5pzMe**) were studied in order to access accurate comparisons in a timely fashion. **2pyMe** was not studied due to its very short half-life.

(28) See the Supporting Information of Ref. 11.

(29) Hill, E. A.; Gross, M. L.; Stasiewicz, M.; Manion, M., *J. Am. Chem. Soc.* **1969**, *91*, 7381-7392.

(30) Wiberg, K. B., *Tetrahedron* **1968**, *24*, 1083-1096.

(31) Noyce, D. S.; Sandel, B. B., *J. Org. Chem.* **1976**, *41*, 3640-3642.

(32) We note that this analysis contrasts with the n-π* nature of the lowest-lying (HOMO → LUMO) electronic transition commonly assigned to E isomer azo photoswitches; the π-π* transition being assigned to higher energies.[2a] The lowest-lying excitation is not always described by a pure HOMO → LUMO monoexcitation. We used TDDFT equations to find the best linear combination of monoexcitations and the corresponding energies. See Ref. 36.

(33) a) Jamorski, C.; Casida, M. E.; Salahub, D. R., *J. Chem. Phys.* **1996**, *104*, 5134-5147. b) Casida, M. E.; Jamorski, C.; Casida, K. C.; Salahub, D. R., *J. Chem. Phys.* **1998**, *108*, 4439-4449. c) Petersilka, M.; Gossmann, U. J.; Gross, E. K. U., *Phys. Rev. Lett.* **1996**, *76*, 1212-1215.

(34) Plater, M. J.; Harrison, W. T. A.; Rzepa, H. S., *J. Chem. Res.* **2015**, *39*, 711-718.

(35) Szabo, A.; Ostlund, N. S. *Modern Quantum Chemistry: Introduction to Advanced Electronic Structure Theory*; Dover Publications, 1989.

(36) Casida, M. E.; Ipatov, A.; Cordova, F. In *Time-Dependent Density Functional Theory*; Marques, M. A. L., Ullrich, C. A., Nogueira, F., Rubio, A., Burke, K., Gross, E. U. K., Eds.; Springer Berlin Heidelberg: Berlin, Heidelberg, 2006, p 243-257.

(37) Cusati, T.; Granucci, G.; Persico, M.; Spighi, G., *J. Chem. Phys.* **2008**, *128*, 194312.

Table of Contents Graphic